ANALYSIS OF THE INFLUENCE OF OUTER ENVELOPE STRUCTURE ON INDOOR THERMAL ENVIRONMENT OF ZERO ENERGY BUILDING

Xiaofei ZHEN[1,2*], Shange LI[1], Jianming PENG[3], Zhouyang Zhao[3], Xu Zhang[1], Chuanxi Tan[1], Ruonan Jiao[1], Wenbing Wu[1], Han Zhan[1]

[1] School of New Energy and Power Engineering, Lanzhou Jiaotong University, Lanzhou 730070, China

[2] Key Laboratory of Railway Vehicle Thermal Engineering of MOE, Lanzhou Jiaotong University, Lanzhou, 730070, China

[3] Lanzhou Zhongjian Construction Technology Limited Liability Company, 730299, China

[*] Corresponding author: zxf283386515@163.com

Zero-energy building is the main development trend in the current construction field. Reducing the carbon emission of the building, enhancing the indoor comfort of the building, and improving the comprehensive performance of the building are the current research hotspots in the field of construction, and it is necessary to explore the impact of the envelope on the performance of the building as the main medium for the transfer of indoor and outdoor heat in the building. In this paper, zero energy consumption buildings in Northwest China are taken as the study application. Numerical simulation and experimental research are combined to compare and analyze the changes of indoor thermal environment under the conditions of external wall insulation layer thickness of 150mm, 140mm, 130mm and window-wall ratio of 0.36 and 0.5 in the heating season. The results show that the indoor comfort level of 130mm is lower than that of 140mm and 150mm external wall insulation layer thickness, and in winter, the increase of window wall ratio improves indoor thermal comfort. In general, increasing the thickness of external wall insulation layer and window wall ratio can be effective means to improve indoor comfort. However, blindly increasing the thickness of insulation layer and window wall ratio will only cause resource waste and cost increase, affecting the long-term development of zero-energy buildings.

Key words: *zero energy building; Outer protective structure; Indoor comfort; Numerical simulation*

1. Introduction

Energy security and environmental friendliness are the premise and basis of sustainable social development. With the rapid economic development and the continuous growth of population, energy crisis and environmental pollution are still the main concerns of the current society [1,2]. Building energy consumption accounts for 22% of total social energy consumption, which is one of the main parts of saving energy and reducing carbon emissions [3,4]. At the same time, building carbon emissions are one of the largest sources of CO_2 emissions, accounting for 35%-50% of total carbon emissions in China, of which 60% comes from the building's operation period, 40% from the construction process, and 2/3 from the main structure and envelope structure [5,6]. Zero-energy buildings can take advantage of the renewable energy resources in and around the building, make the annual renewable energy capacity greater than or equal to the total energy consumption of the building throughout the year, which is the main research and development direction of the field of architecture [7,8].

People spend between 85% and 90% of their time indoors on average [9,10], whether indoor comfort is good or not will affect the physical and mental health of residents. With the progress of living quality, people's requirements for indoor thermal comfort are also gradually increasing. The research on the indoor comfort of buildings has been widely concerned by scholars [11,12].

Some studies have investigated the indoor thermal environment and air conditioning supplementary heating behavior of the user's residence in winter, the temperature distribution in different areas of the residence is analyzed and the corresponding heating system optimization scheme is proposed [13]. A team conducted a practical test on the indoor thermal environment of a traditional house in a rural area, evaluated and analyzed the test results combined with the PMV-PPD human comfort index, and proposed improvement method according to the evaluation results [14]. Some utilized a questionnaire survey, a field test, and a simulation, the studies summed up the problems with the indoor light environment, heat and humidity environment, and air quality of a university classroom in Xi'an, as well as the rules regarding the way such conditions change over time and space. They also suggested methods to address the problems based on the outdoor climate of the area [15]. Some used Airpark software to simulate and analyze a postgraduate studio in Jinan City, and the distribution of indoor temperature and humidity is obtained. The results could provide theoretical methods and comparative analyses for the indoor comfort of similar office buildings [16]. A team used Design Builder software to analyze the residential thermal environment, and the results indicated that a simple outer envelope structure and a single material were the main reasons for natural ventilation buildings' poor indoor thermal environment. The author added thermal insulation materials to the envelope structure and hollow glass windows, along with other optimization strategies. The overall thermal environment rating of the residence was improved by 4.7% after optimization. [17]. Some studies have analyzed the annual changes of residential indoor thermal environment and the corresponding influencing factors, and combining with computer simulation of the changes of indoor thermal comfort under three optimal working conditions, an optimal solution is finally determined [18]. Researchers developed thermal energy storage cement mortar (TESCM) and explored the thermophysical properties, microstructure, and spectral properties of CS-ECPCM. The test results showed that the phase transition temperature and latent heat of CS-ECPCM were 23.67°C and 24.43 J/g, respectively, and the structure of the calcium carbonate encapsulated TESCM was enhanced, which led to the compressive strength of TESCM to be decreases, in addition, its thermal conductivity decreases with the increase of CS-ECPCM dosage, which leads to the effective improvement of its thermal insulation performance. [19].

At present, scholars mainly focus on the internal comfort of ordinary building rooms and the corresponding improvement measures, while zero-energy buildings are defined as buildings with renewable energy greater than or equal to their own energy consumption, so their key technologies are how to save energy or maximize production capacity, but there is a lack of relevant research on the distribution of indoor temperature and humidity.

This paper takes the office building with zero energy consumption as the research object

(Hereinafter referred to as Zhongjian Building), and the parameters of indoor hygrograph and wind speed in heating season were tested experimentally. CFD software was used to emulate and investigate the thermal environment inside the room under different insulation thicknesses and window-wall ratios, and the room interior comfort was evaluated with PMV-PPD evaluation index. The influence of insulation layer thickness and window-wall ratio on the room interior thermal environment of buildings was studied. This study can provide reference for the design of zero-energy building envelope structure in different areas, and has a positive effect on the application and advancement of zero-energy buildings.

2. Research Methods

In this study, experiment and numerical simulation are used to analyze the distribution of temperature, humidity and wind speed in zero-energy architectures under different external wall insulation thicknesses as well as different window -wall ratios. The route of the paper is shown in Fig. 1.

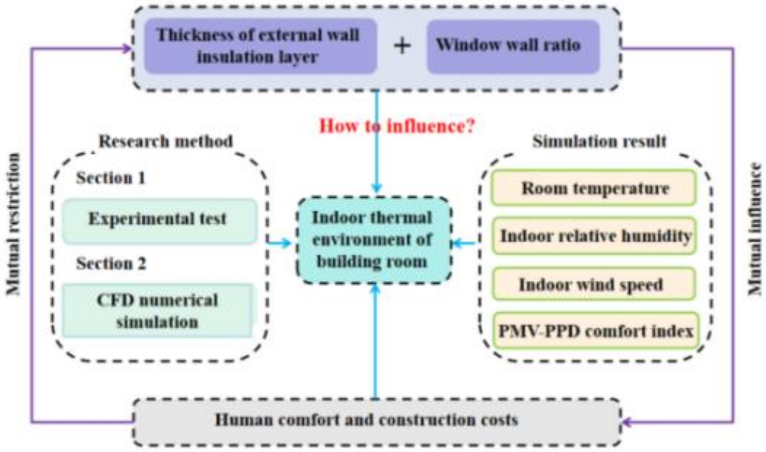

Fig. 1. Research content and ideas

2.1. Introduction of research objects

Zhongjian Building is located in Lanzhou City, Gansu Province, with a construction area of 2270.01m^2, four floors above ground, body shape coefficient of 0.31, east window wall area ratio of 0.05, west window wall area ratio of 0.04, north window wall area ratio of 0.34, and south window wall area ratio of 0.24. The building fully considers the local climate conditions and natural resources, the use of efficient lighting, efficient energy-saving evaporative chiller, plate heat exchanger energy-saving measures, low temperature air source heat pump energy-saving measures, mechanical ventilation heat recovery, tunnel air precooling and other active technologies, among which the envelope structure is made of air tightness envelope materials with high thermal insulation performance [20].

2.2. Indoor thermal environment experimental test

Geographical location and meteorological conditions are the main factors affecting the thermal environment of buildings [21,22]. The hourly meteorological parameters of Lanzhou from December 10 to March 31 are shown in Fig. 2 and Fig. 3.

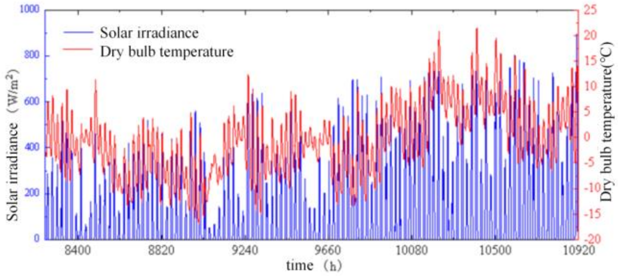

Fig. 2. Hourly solar radiation and temperature

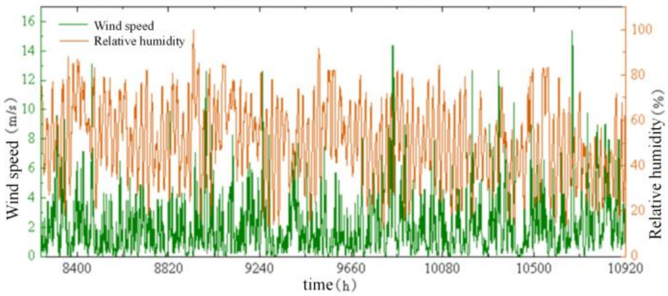

Fig. 3. Outdoor hourly wind speed and relative humidity

The winter in Lanzhou is long and cold, it has a large diurnal temperature difference. The mean temperature of the whole heating season is about -1℃, the mean wind speed is 2m/s, and the mean relative humidity is 52%. The lowest temperature reached -16.8℃ at 7 am on January 11, when the wind speed was 1m/s and the relative humidity was 80%.

Study of envelope effects on indoor comfort in extreme weather conditions more extensive. For example, the indoor thermal environment distribution of buildings under extreme weather conditions in heating season has been studied [23,24]. The minimum temperature of -16.8℃ and the corresponding wind speed and relative humidity at that time were input into the Airpark software as boundary conditions, and other boundary conditions were set accordingly to study and analyze the indoor temperature, humidity and wind speed distribution of the zero-energy building.

There are many rooms in Zhongjian Building, some of which are non-office rooms, and the building faces south, so the northwest corner office of each floor on floors 1-3 is selected for data collection in this test. During the test, the side door on the first floor of the office building was opened, but the main door of the hall and all other doors and windows in the building were closed. There were no disturbance in any other rooms except the test room, which had 4 people, the tunnel air and fresh air heat recovery system were opened.

Temperature and humidity data were collected for 111 consecutive days from December 10 to March 31, and the data was recorded every hour. The measuring points were evenly arranged in the middle of each room at a height of 1.7m. The main experimental instruments used during the test are shown in Tab.1.

Tab.1. Testing instrument

Name	Producer	Accuracy	Type
Temperature and humidity recorder	The Big Dipper	±0.1℃ ±3%RH	NB-IoT wireless temperature and humidity

Based on the test data in Fig. 4 and Fig. 5, the average temperature of rooms 101, 201 and 301 is 21.64℃, 23.06℃ and 21.94℃ respectively, and the average humidity is 36.55%, 31.32% and 34.28% respectively. In the heating season, more than 2/3 of them meet the requirements of indoor thermal environment standards [25].

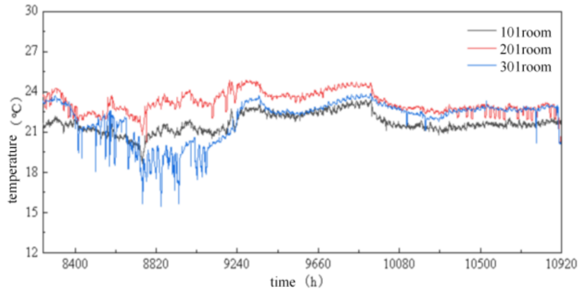

Fig. 4. Indoor hourly temperature by measuring

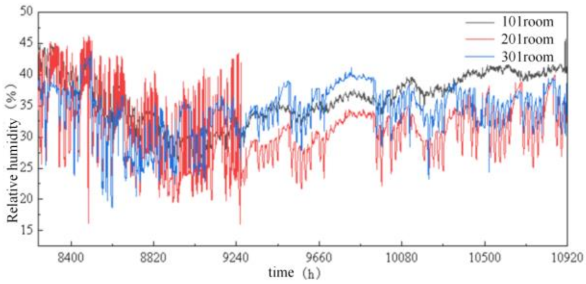

Fig. 5. Indoor hourly relative humidity by measuring

2.3. Physical model establishment

It is not realistic to analyze indoor thermal environment under different working conditions by experimental method [26,27], by changing the parameters of the envelope structure in a software, the influence of the envelope structure on intra-room thermal environment can be emulated and analyzed. In this paper, the Northwest corner office on the 2nd floor is selected and the physical modeling is carried out in Airpark software.

The room is equipped with 4 computers, 4 desks and 4 staff, the staff are in a sitting state, the air outlet is set at the top of the east wall and the ceiling near the window side position, in addition, a 35℃ heat source is set on the floor instead of the air source heat pump in the room, the south window wall ratio is 0.24, the door is set in the north wall.

The 4mm SLATE glass fiber reinforced polyester tire + 3mmPE glass fiber tire + 150mm extruded polystyrene board + 200mm reinforced concrete roof board are used for roof construction, and the south wall (exterior wall) adopts 15mm finishing paint + 5mm plastering paste + 150mm rock wool insulation layer + 10mm cement mortar + 15mm finishing mortar + 200mm base wall. The east, west and north walls (interior walls) are made of 15mm finishing paint + 5mm plastering mortar + 50mm rockwool insulation layer + 10mm cement mortar + 15mm finishing mortar + 200mm base wall. As shown in Tab.2. The composition of wall materials is shown in Fig. 6.

Tab.2. Basic parameter settings

Name	Size and construction	Boundary condition	Operating parameter
Typical room	7.75m×6.95m×3.97m	—	—
Door	1.5m×2.4m	—	Heat transfer coefficient 0.9W/ (m2.K)
Window	1.8m×2m	Constant heat transfer coefficient	Heat transfer coefficient 0.8W/ (m2.K)
Air supply outlet	0.5m×0.2m	Velocity inlet, 1m/s	—
Return air opening	0.5m×0.2m	Free export	—
Personnel (4)	0.4m×0.3m×1.75m	75W	—
Computer (4)	0.4m×0.3m×0.3m	150W	—
Desk (4)	1.5m×0.5m×1m	Adiabatic	

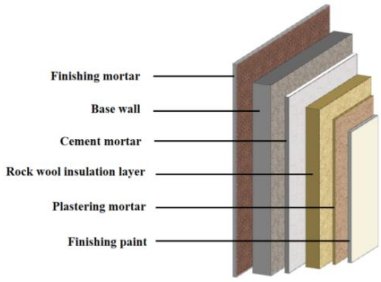

Fig. 6. Wall structure

2.4. Mathematical model

The zero equation model refers to the turbulent viscosity as a function of local mean velocity and length scale [28,29]. Compared with k-ε turbulence model, it is more converging and accurate in dealing with indoor problems, and has a high agreement with experimental results. Airpark software is also based on the zero equation model, and adopts the finite volume method to obtain the distribution of temperature, humidity, velocity and pressure at various positions in the flow field through the continuity equation, energy conservation equation and momentum conservation equation of fluid flow [30,31]. The outer insulation layer of the room is made of polystyrene board material. In addition, since the temperature in the area where the research object is located is the lowest on January 11, 2022, reaching -16.8°C, at which time the wind speed is 1 m/s, and the relative humidity is 80%, the boundary conditions of the CFD simulation are also set in this way. Also, the following assumptions need to be made in the simulation calculations.

(i) The flow of indoor air is steady flow.

(ii) The radiative heat transfer between the envelope and indoor objects is neglected.

(iii) Ignoring the effects of cold air infiltration through doors and windows.

(iv) The physical parameters of the fluid and the interior structure keep constant.

In order to simplify the simulation calculation, it is assumed that the air inside the building room is an incompressible fluid [32,33]. Based on the above assumptions, the air flow in the building room follows the governing equations [34,35].

(1) Continuity equation

$$\frac{\partial \rho U_i}{\partial X_i}=0 \tag{1}$$

Where U_i denotes the mean velocity component in the X_i direction and denotes the air density.

(2) Momentum equation

$$\frac{\partial \rho U_i}{\partial t}+\frac{\partial \rho U_i U_j}{\partial X_i}=-\frac{\partial P}{\partial X_i}+\frac{\partial}{\partial X_j}(\mu(\frac{\partial U_i}{\partial X_j}+\frac{\partial U_j}{\partial X_i})-\rho U_i U_j) \tag{2}$$

Where: represents the average velocity component in the direction, and respectively represent the pulsation velocity component, stands for air pressure,expressed dynamic viscosity.

(3) Energy equation

$$\frac{\partial \rho H}{\partial t}+\frac{\partial(\rho \mu_j H)}{\partial X_j}=\frac{\partial}{\partial X_j}(\frac{k}{c_p}\frac{\partial T}{\partial X_j}-\rho \mu_j H') \tag{3}$$

Where: and represents static enthalpy and pulsating static enthalpy, represents the specific heat capacity at constant pressure.

3. Model verification

In order to explore the optimal grid size and reserves of the model, the grid division of the model was adjusted and simulated for many times. The data of five kinds of grid quantities with the maximum grid size of 50mm, 60mm, 70mm, 90mm and 120mm at the same position were compared, and the corresponding grid numbers were shown in Tab.3. The temperature data of points 1 and 2 were selected to verify the grid independence of the simulation, where points 1 and 2 were the measurement points with the height of 0.5m and 1.7m in the center of the room, respectively.

Tab.3. Temperature comparison of maximum mesh size and mesh number

Maximum mesh size(mm)	Grid number	Temperature at point 1(℃)	Temperature at point 2(℃)
120	480863	29.95	28.5
90	827869	29.32	28.12
70	1425861	29.04	28.03
60	2003620	29.03	28.01
50	3152465	29.03	28.01

As can be seen from Fig. 7, when the maximum mesh size is reduced to 70mm and the number of grids is 142w, the temperature data will not be reduced, so the mesh size of 70mm is used for subsequent simulation.

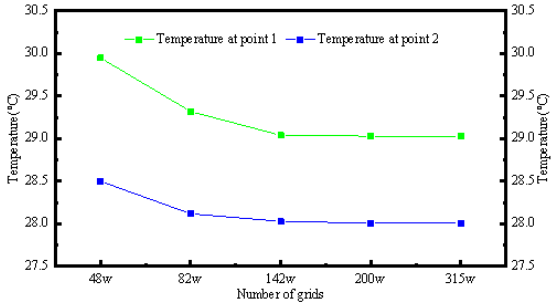

Fig. 7. Grid independence verification

After the grid independence was verified, the accuracy of the physical model was verified. Four measurement points, A, B, C and D, were selected horizontally at a height of 1.7 m in the room, and the experimental and simulated values of temperature and humidity at these points were compared one by one, as shown in Tab.4.

Tab.4. Comparison of tested and simulated values

point	Temperature (°C)		Relative humidity (%)	
	experimental	analogue	experimental	analogue
A	23.06	24.26	32.32	32.86
B	23.15	23.41	31.12	32.32
C	24.21	25.12	30.85	31.23
D	23.22	24.12	31.26	32.21

As can be seen from the above table, the four measurement points temperature simulation value and the measured value of the largest error value at point A, the error value of 4.9%, the smallest error of 1.1% at point B; the maximum error value of relative humidity is 3.7%, the simulation value of the above measurement points and the measured value of the error is within 5%, within the error allowable range. Therefore, the established physical model has good reliability and can be used for further investigation.

4. Simulation results

The thickness of insulation layer and the ratio of window to wall are two main reasons affecting the room interior thermal environment [36,37]. The intra-room thermal environment under the thickness of 150mm, 140mm and 130mm external wall insulation layer and the southward window to wall ratio of 0.36 and 0.5 under the condition of 150mm were simulated and analyzed respectively. Since most of the time, indoor staff conduct office activities in sitting position, the perceived temperature zone above the head of the indoor staff is about 1.7m above the ground, and the thermal comfort zone of the legs is about 0.6m above the ground [38,39].

4.1. First option

The first envelope scheme is the simulation of indoor thermal comfort when the thickness of the insulation layer is 150 mm and the south-facing window-to-wall ratio is 0.24, as shown below.

As can be seen from the Fig. 8, when people are sitting, because there is floor heating in the room (instead of air source heat pump), the indoor temperature is generally about 23.2℃ while the wind speed at this time is about 0.05m/s-0.1m/s, and the wind speed at the location of computers and personnel is slightly larger than that in other areas. When Z=1.7m, the average indoor temperature is about 22.5℃, the temperature is more comfortable, the wind speed is larger than that when Z=0.6m, the relative humidity of air in Z=0.6m and Z=1.7m is about 32%, and the south wall (with Windows) is in direct contact with the external environment, the temperature at both heights is low.

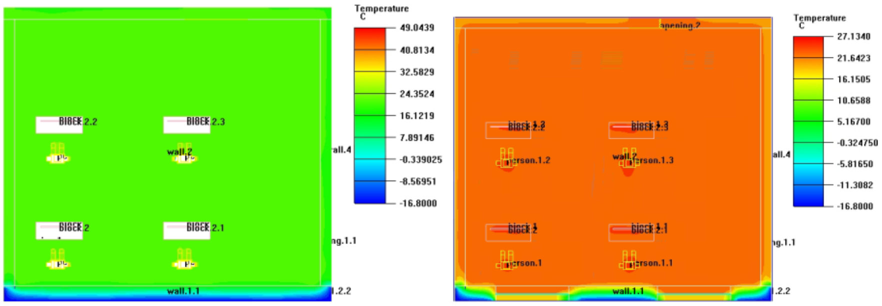

(a) Z=0.6m Temperature cloud map (b) Z=1.7m Temperature cloud map

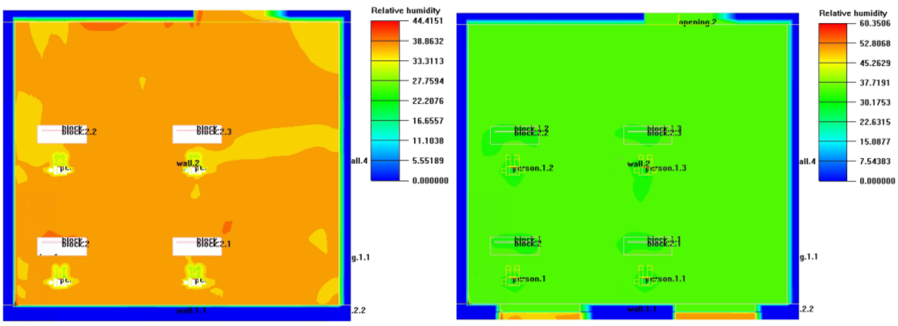

(c) Z=0.6m relative humidity cloud map (d) Z=1.7m relative humidity cloud map

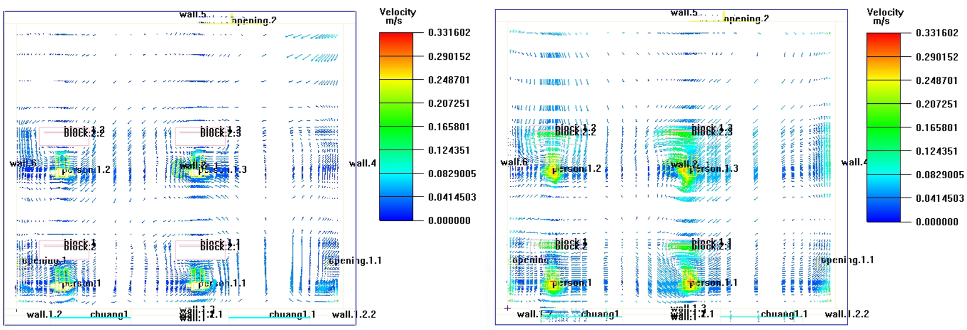

(e) Z=0.6m velocity vector cloud map (f) Z=1.7m velocity vector cloud map

Fig. 8. Vector cloud map of temperature, relative humidity and wind speed

PMV-PPD comfort index is an index proposed by Professor Fanger in Denmark to characterize human thermal response, while the percentage of dissatisfaction predicted by PPD is to make up for the incompleteness of PMV index value. When PMV value is between -1 and 1, human comfort is good when PPD is within 20% [40,41]. From Fig. 9, it can be observed that the PMV values at two heights of 0.6m and 1.7m are -0.8 and 0.3 respectively, and the PPD values are less than 20%, it can be seen that the indoor comfort of the building under this condition meets the human thermal comfort requirement.

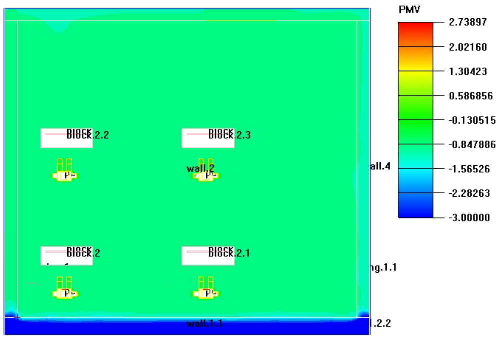

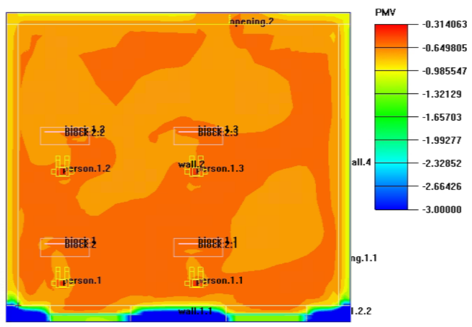

(a) Z=0.6mPMV cloud map (b)Z=1.7mPMV cloud map

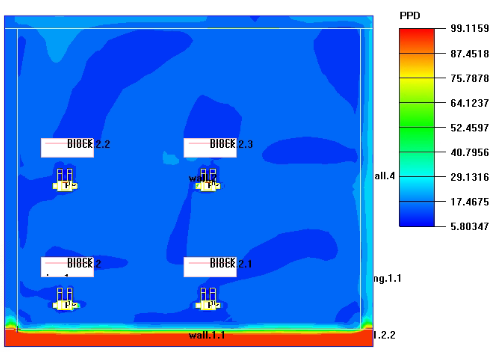

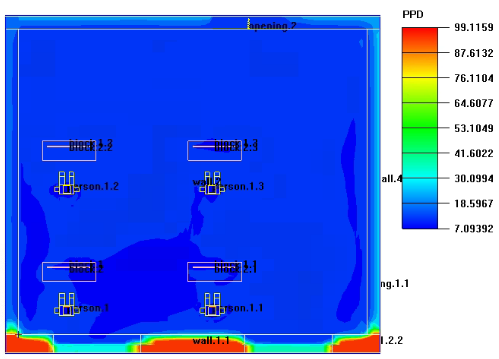

(c) Z=0.6mPPD cloud map (d) Z=1.7mPPD cloud map

Fig. 9. PMV-PPD index cloud map

4.2. Second option

The second envelope scheme is the simulation of indoor thermal comfort when the thickness of the insulation layer is 140 mm and the south-facing window-to-wall ratio is 0.24, as shown below.

As can be seen from the Fig.10, after the thickness of the external wall insulation layer is reduced by 10mm, the indoor temperature at the height of 0.6m is reduced from 23.2°C to about 22.3°C, and the room internal temperature at an altitude of 1.7m is reduced from 22.5°C to about 21.6°C, both of which decrease by about 1°C. The relative humidity changes from 32% to 35%, and the changes can be ignored.

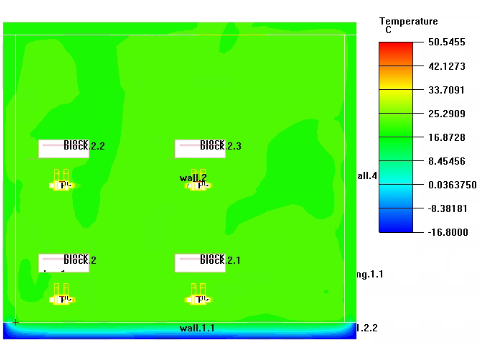

(a) Z=0.6m Temperature cloud map

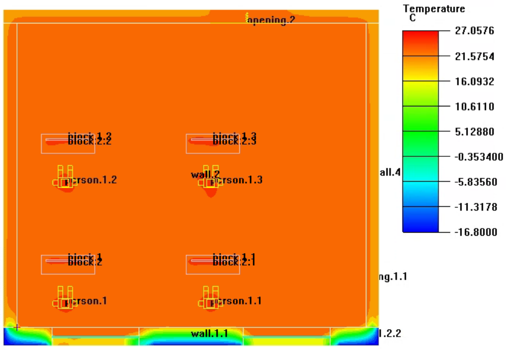

(b)Z=1.7m Temperature cloud map

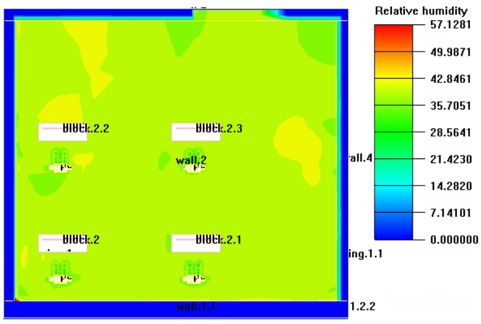

(c) Z=0.6m relative humidity cloud map

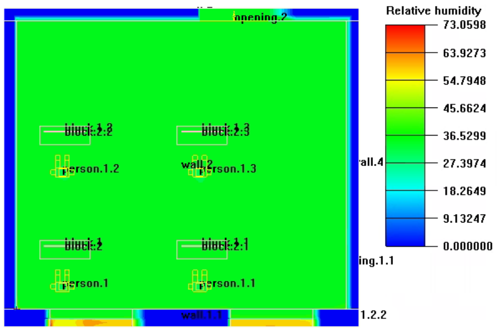

(d) Z=0.6m relative humidity cloud map

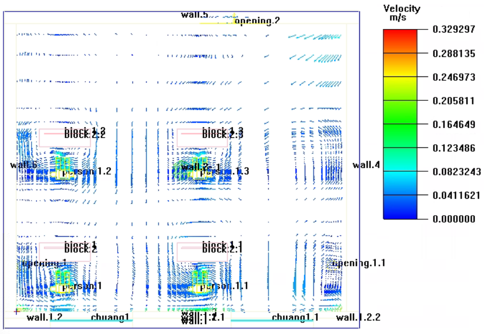

(e) Z=0.6m velocity vector cloud map

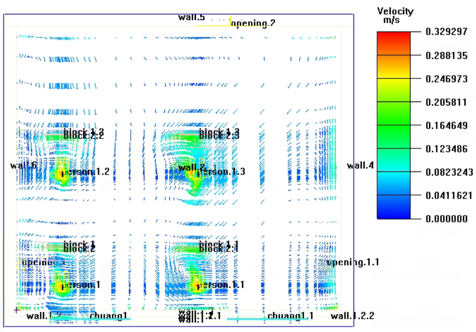

(f) Z=1.7m velocity vector cloud map

Fig. 10. Vector cloud map of temperature, relative humidity and wind speed

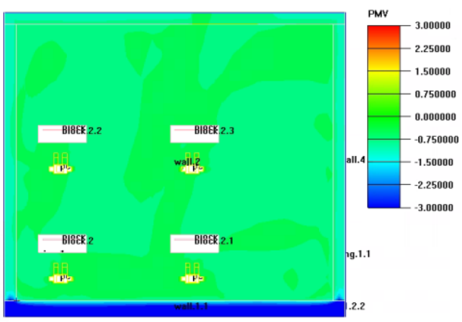

(a) Z=0.6mPMV cloud map

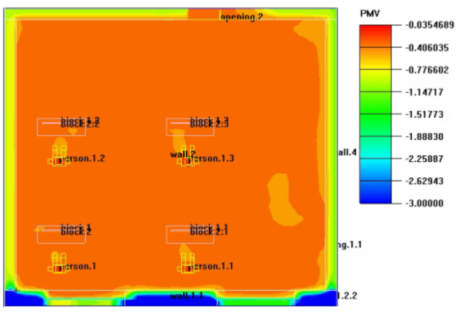

(b) Z=1.7mPMV cloud map

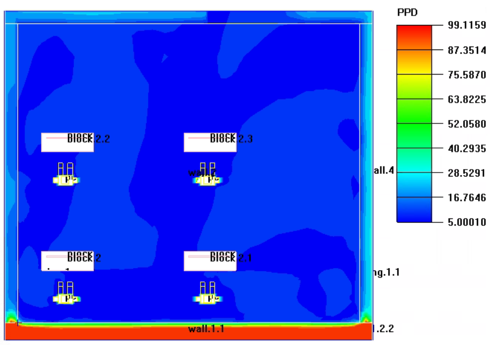

(c) Z=0.6mPPD cloud map

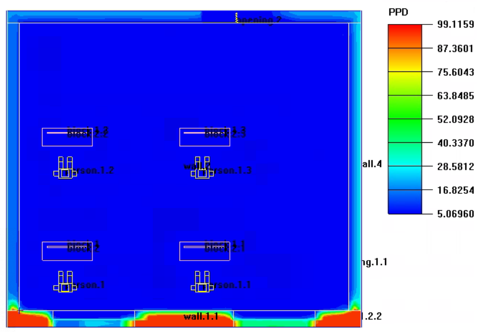

(d) Z=1.7mPPD cloud map

Fig. 11. PMV-PPD index cloud map

As can be seen from the Fig.11, from the PMV-PPD index distribution at the two heights, it can be seen that after the thickness of the insulation layer is reduced from 150mm to 140mm, except for the position near the wall and the window, the degree of human dissatisfaction in the remaining space is still less than 20%, and the human comfort level has little change.

4.3. Third option

The third envelope scheme is the simulation of indoor thermal comfort when the thickness of the insulation layer is 130 mm and the south-facing window-to-wall ratio is 0.24, as shown below.

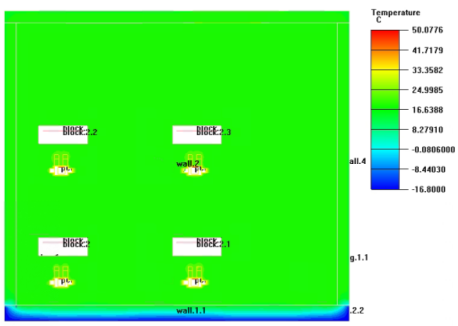

(a) Z=0.6m Temperature cloud map

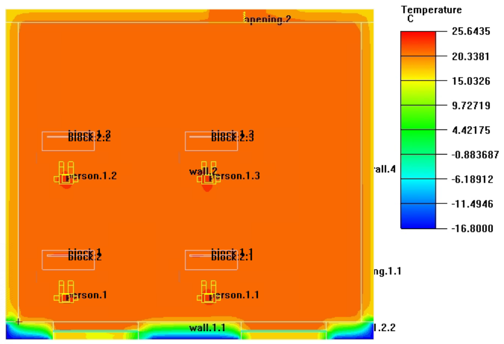

(b) Z=1.7m Temperature cloud map

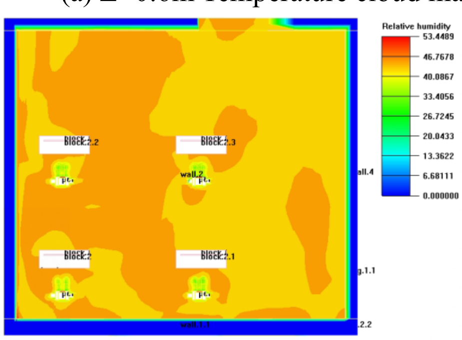

(c) Z=0.6m relative humidity cloud map

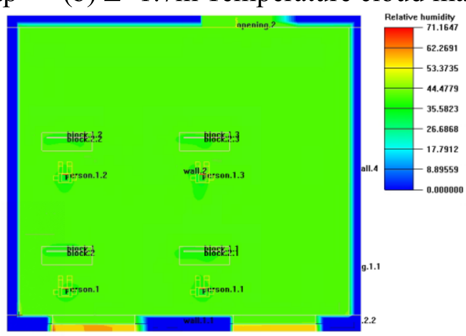

(d) Z=1.7m relative humidity cloud map

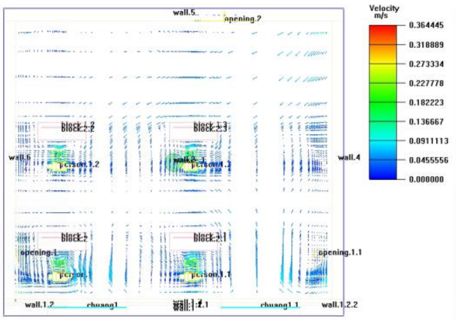
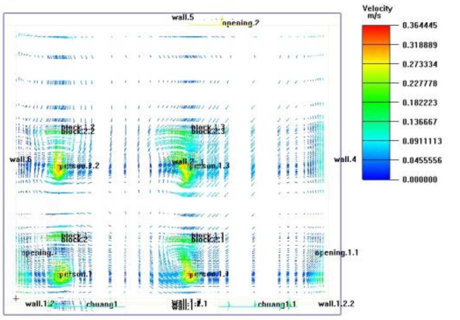

(e) Z=0.6m velocity vector cloud map (f) Z=1.7m velocity vector cloud map

Fig. 12. Vector cloud map of temperature, relative humidity and wind speed

As can be seen from the Fig.12, after the thickness of external wall insulation layer is reduced from 140mm to 130mm, the room internal temperature is reduced to about 18.5 °C compared with 140mm and 150mm insulation layer thickness, the temperature is reduced by 3°C and 5°C, respectively. At a height of 1.7m, the relative humidity increased by 4% and 7%, and the wind speed increased by 0.06m/s and 0.08m/s, respectively.

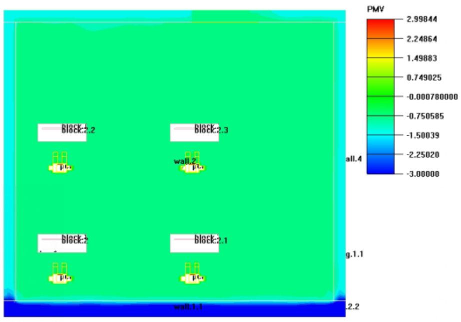
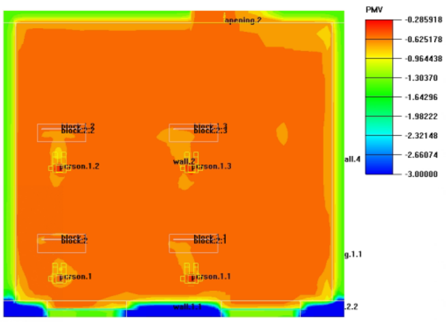

(a) Z=0.6mPMV cloud map (b) Z=1.7mPMV cloud map

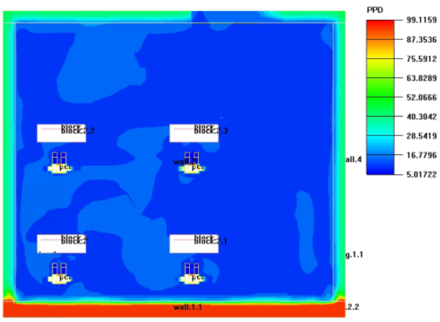
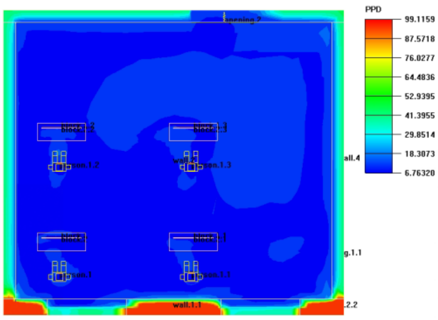

(c) Z=0.6mPPD cloud map (d) Z=1.7mPPD figure loud map

Fig. 13. PMV-PPD index cloud map

Based on the Fig.13, the PMV-PPD index cloud map, as the thickness of the insulation layer on the external wall decreases, correspondingly decreases the level of human comfort. This means that the level of human dissatisfaction rises, but it is still within the acceptable range for the human body. This means that the PMV value is between -1 and 1, and the index value is below 20%; however, the range of human comfort is noticeably lower compared with the previous two kinds of insulation layer thickness.

4.4. Fourth option

As can be seen from the Fig.14, the fourth envelope scheme is the simulation of indoor thermal comfort when the thickness of the insulation layer is 150 mm and the south-facing window-to-wall ratio is 0.36, as shown below.

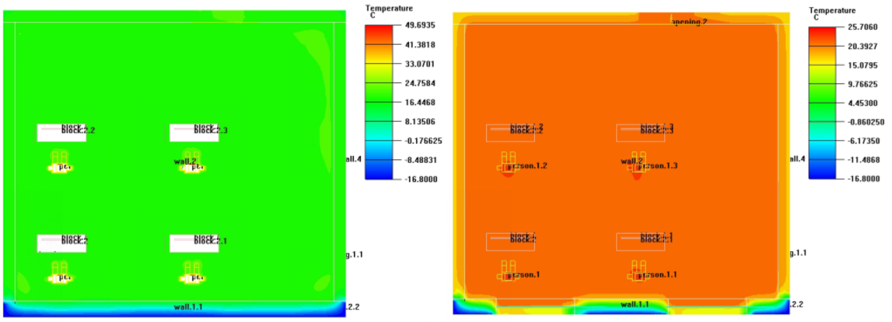

(a) Z=0.6m Temperature cloud map (b) Z=1.7m Temperature cloud map

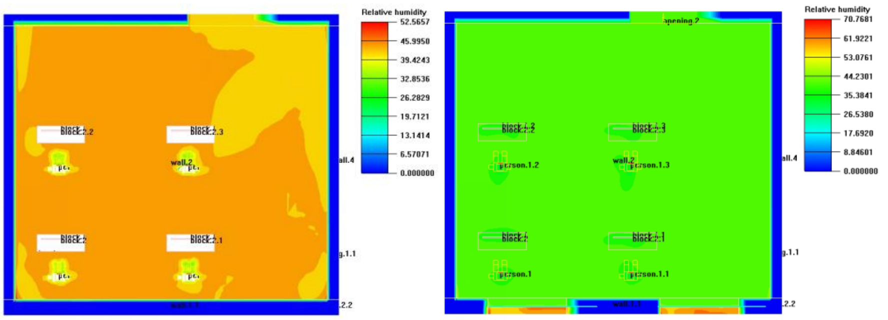

(c) Z=0.6m relative humidity cloud map (d) Z=1.7m relative humidity cloud map

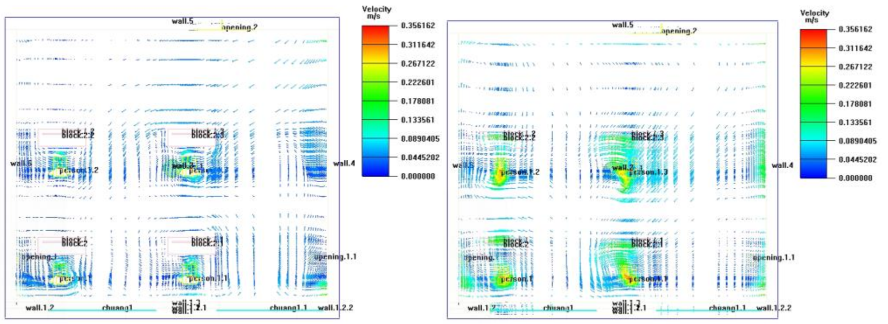

(e) Z=0.6m velocity vector cloud map (f) Z=1.7m velocity vector cloud map

Fig. 14. Vector cloud map of temperature, relative humidity and wind speed

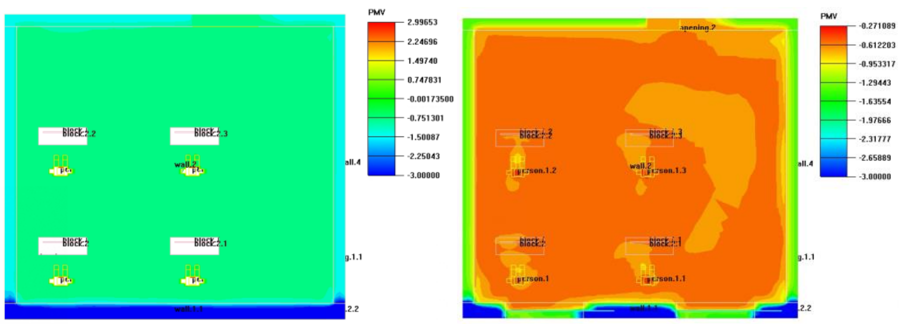

(a) Z=0.6mPMV cloud map (b) Z=1.7mPMV cloud map

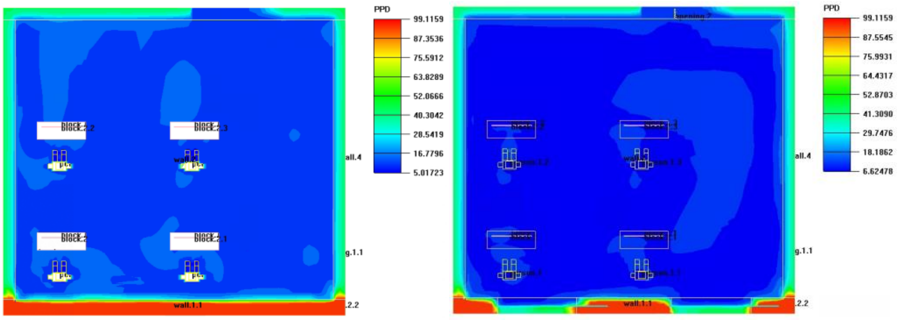

(c) Z=0.6mPPD cloud map (d) Z=1.7mPPD cloud map

Fig. 15. PMV-PPD index cloud map

As can be seen from the Fig.15, when the window wall ratio increased from 0.24 to 0.36, the indoor temperature increased by about 2℃, and the relative humidity decreased from 32% to about 30%. According to the PMV-PPD index value, human comfort is slightly improved.

4.5. Fifth option

As can be seen from the Fig.16, the fifth envelope scheme is the simulation of indoor thermal comfort when the thickness of the insulation layer is 150 mm and the south-facing window-to-wall ratio is 0.5, as shown below.

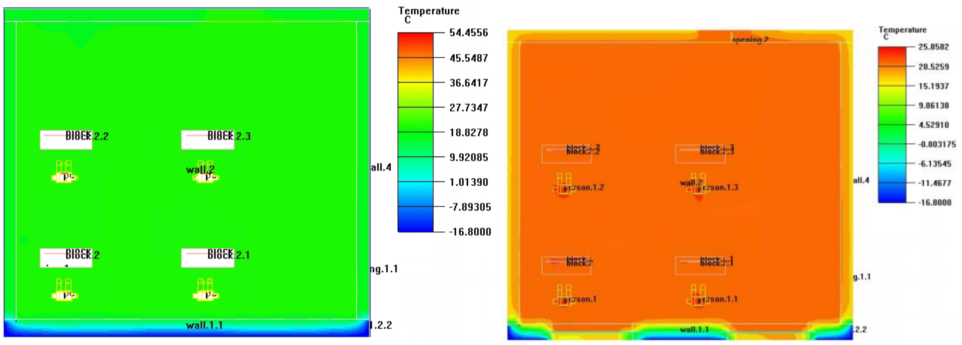

(a) Z=0.6m Temperature cloud map (b) Z=1.7m Temperature cloud map

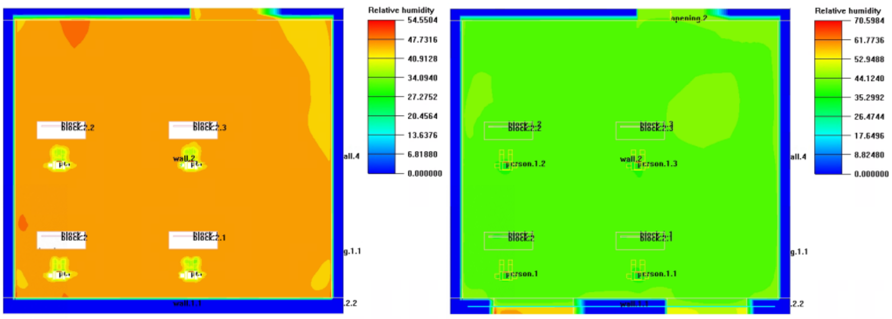

(c) Z=0.6m relative humidity cloud map (d) Z=1.7m relative humidity cloud map

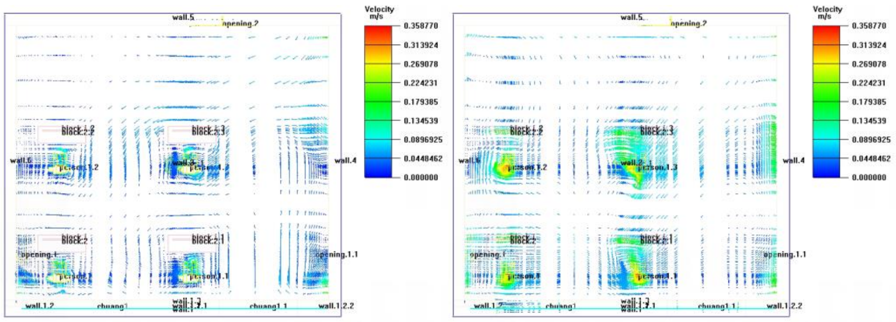

(e) Z=0.6m velocity vector cloud map (f) Z=1.7m velocity vector cloud map

Fig. 16. Vector cloud map of temperature, relative humidity and wind speed

When the window-wall ratio is increased to 0.5, the temperature is observed to be slightly higher than previous two window-wall ratio conditions for the heights of 0.6 m and 1.7 m.

According to the change of PMV-PPD index values shown in Fig.17, indoor comfort increases when the window-wall ratio is increased to 0.5. The reason maybe that an increase in the window-wall ratio of the south wall can increase the amount of solar radiation, which makes indoor sunlight more abundant, and thus the indoor comfort is effectively improved in winter.

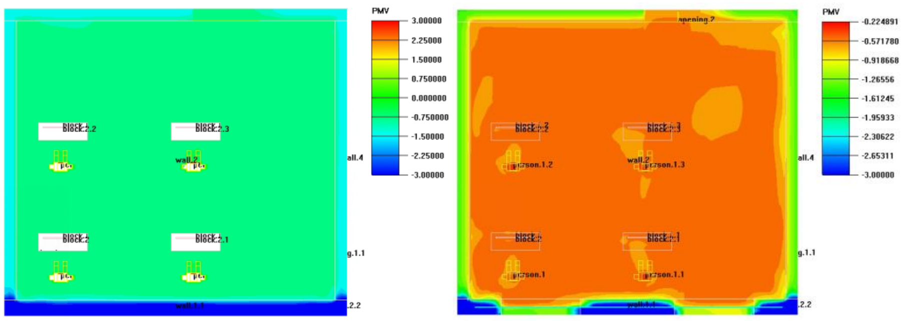

(a) Z=0.6mPMV cloud map (b) Z=1.7mPMV cloud map

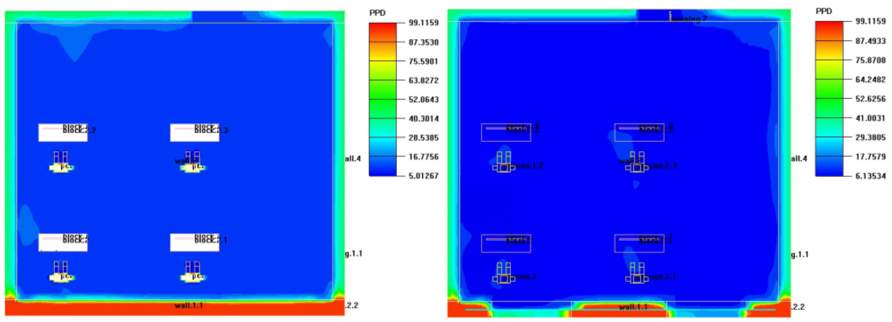

(c) Z=0.6mPPD cloud map (d) Z=1.7mPPD cloud map

Fig. 17. PMV-PPD index cloud map

5. Conclusion

In this paper, a test and numerical simulation approach are proposed to study the influence of external wall insulation layer thickness and the window-wall ratio on the indoor thermal environment of zero-energy buildings in Northwest China. The following are the main conclusions.

(1) In general, increasing the thickness of the insulation layer can improve indoor comfort; nevertheless, it is discovered that changing the thickness of the insulation layer by 10mm has very little influence on intra-room thermal environment index value and comfort. Therefore, a waste of economic cost/resources may be caused when the thickness of the external wall insulation layer is blindly increased. For better develop zero-energy buildings, the insulating material and its thickness should be appropriately selected according to the geographical environment and natural resources of the location.

(2) It is demonstrated that the window-wall ratio is one of the main influential factors that affecting the indoor thermal environment. Similarly, the window-wall ratio of the building should be rationally selected considering the geographical environment and climatic conditions of the area in order to avoid resources waste and high economic cost.

Acknowledgements

This work was funded by the National Natural Science Foundation of China (52206255), the Youth Science and Technology Talent Lift Program of Gansu Province (GXH20220530-14), the Youth Science Foundation Project of Lanzhou Jiaotong University (2020018, 2020011), the Gansu Province Youth Science Fund project (No. 22JR11RA148), and Department of Housing and urban-rural Development of Gansu Province (JK2023-49).

Nomenclature			the dynamic viscosity (Pas)
PMV-PPD	Human Thermal Comfort Evaluation Indicators	*t*	time (s)
k	turbulent kinetic energy of a fluid (J)	*P*	air pressure (Pa)
	air density (kg/m3)	T	Temperature (°C)
	average velocity component in the X_i direction		average velocity component in the X_j direction
H	the static enthalpies (J)	*H'*	pulsatile static enthalpies (J)

References

[1] Biswas, S., et al., Kar S. Energy Efficiency and Environmental Sustainability: A Multi-Criteria based Comparison of BRICS and G7 Countries//Emerging Technology and Management Trends in Environment and Sustainability: Proceedings of the International Conference, EMTES-2022. Taylor & Francis, 2023: 107.

[2] Li, B. Y., et al., Energy consumption pattern and indoor thermal environment of residential building in rural China. Energy and Built Environment, 2020, 1(3).

[3] Tan, Z. J., et al., A comparative study of building energy efficiency standards between China and Japan in the context of carbon neutrality. Building Science, 2023, 39(02): 171-182+214.

[4] Gou, Y. Y., Evaluation of efficiency of energy saving renovation of existing residential buildings based on value engineering. Qingdao University of Technology, 2022.

[5] Pen, C., et al., Low carbon buildings and low carbon cities. Beijing: China Environmental Science Press, 2018:3-15.

[6] Wu, R. Q., Research on ecological design of office building envelope based on data analysis and evaluation. North China University of Technology, 2022.

[7] Chen, J., et al., Research on the application and popularization mode of zero energy building technology in hot summer and warm winter area. Construction Science and Technology, 2019(24): 25-27.

[8] Lin, Y., et al., Towards zero-energy buildings in China: A systematic literature review. Journal of Cleaner Production, 2020, 276: 123297.

[9] Ganesh G A, Sinha S L, Verma T N, et al. Investigation of indoor environment quality and factors affecting human comfort: A critical review. Building and Environment, 2021, 204: 108146.

[10] Kapoor, N. R., et al., A Systematic Review on Indoor Environmental Quality in Naturally Ventilated School Classrooms: A Way Forward. Advances in Civil Engineering, 2021.

[11] Song, J. F., et al., Study on retrofitting design of Hongjiang sub-scenting house in Yuanshui River Basin[J/OL]. Journal of Changsha University of Science & Technology (Natural Science), 2023, 20(3):1-2.

[12] Chen, X. M., et al., Remote sensing of indoor thermal environment from outside the building through window opening gap by using infrared camera. Energy & Buildings, 2023, 286.

[13] Yin, P., et al., Winter indoor thermal environment and heating demand of low-quality centrally heated houses in cold climates. Applied Energy, 2023, 331: 120480.

[14] Yu, Z. C., Men, Y. H., Test and analysis of indoor thermal environment and energy consumption of rural residential buildings in Guanzhong area of Shaanxi Province in summer. Building Energy Efficiency, 2018, 46(1): 39-46.

[15] Shi, B. C., Research on the indoor physical environment of university classrooms in Xi 'an based on comfort. Chang’an University, 2021.

[16] Rong, C. L., Numerical simulation of indoor thermal environment in studio based on Airpak software. Contamination Control & Air-Conditioning, 2021(02): 50-53.

[17] Zheng, W., et al., Effect of the envelope structure on the indoor thermal environment of low-energy residential building in humid subtropical climate: In case of brick–timber vernacular dwelling in China. Environmental Technology & Innovation, 2022, 28: 102884.

[18] Grudzińska, M., Optimization of balcony's glazed enclosure with spectrally selective coatings regarding heating demand and thermal comfort in a multifamily building. International Journal of Energy and Environmental Engineering, 2022: 1-16.

[19] Kaushik, N., et al., Thermal analysis of a double-glazing window using a Nano-Disbanded Phase Changing Material (NDPCM). Materials Today: Proceedings, 2022, 62: 1702-1707.

[20] Peng, J. M., et al., Demonstration research and practice of net zero energy building in cold area -- Office building # 1, Zhongjian Building Project, Lanzhou New Area. Construction Science and Technology, 2020(12): 55-60.

[21] Ren, K., Study on indoor thermal environment optimization design of existing residential buildings in Nankang New Village, Xi 'an. Xi'an University of Architecture and Technology, 2022.

[22] Li, D. X., et al., Comparison of air conditioning forms of a near zero energy residential building in Hangzhou. Heating Ventilating & Air Conditioning, 2023, 53(06): 75-84.

[23] Jiang Z H. Study on energy saving renovation design of rural residential buildings in hot summer and cold winter areas. Anhui Jianzhu University, 2022.

[24] Roque, E., et al., The Impact of Thermal Inertia on the Indoor Thermal Environment of Light Steel Framing Constructions. Energies, 2022, 15(9).

[25] GB/T 50785-2012. Evaluation standard for indoor heat and humidity environment of civil buildings.

[26] Ding, Y., et al., Optimization of air flow organization based on improvement of indoor thermal environment of existing public buildings. Heating Ventilating & Air Conditioning, 2023, 53(06): 150-155+170.

[27] Liu, L., Study on indoor thermal environment test and simulation of rural residential buildings in Guanzhong area. Xi'an University of Architecture and Technology, 2022.

[28] Ma, J., et al., Analysis of influence of exhaust air on inlet air of indirect evaporative cooling chiller in Xi 'an area based on Airpak. Refrigeration & Air Conditioning, 2023, 37(02): 297-304.

[29] Li, Y., et al., Numerical simulation analysis of thermal environment in office of cabinet air conditioner in summer based on Airpak. Journal of North China University of Technology, 2017, 29(02): 122-130.

[30] Wang, Z., Dong, M., Numerical simulation of inlet pipe assembly structure optimization of shell-and-tube heat exchanger based on Fluent. Modern Information Technology, 2022, 6(20): 111-115.

[31] Yang, Y. J., et al., Simulation study on the effect of cold radiant panel layout on office thermal environment. Fluid Machinery, 2017, 45(01): 77-81+19.

[32] Liu, X., et al., Analysis on the influence of air supply mode of air conditioner on indoor thermal environment based on Airpak. Journal of Anhui Institute of Architecture & Industry, 2019, 27(01): 70-75.

[33] Liu, Y. J., et al., Air flow organization optimization of air-conditioned room based on BIM coupled ANSYS-Fluent simulation technology. Architecture Technology, 2023, 54(08): 934-939.

[34] Gong, X., Jiang, Q. H., Numerical simulation analysis of office thermal environment based on Airpak. Journal of Information Technology in Civil Engineering and Architecture, 2019, 11(6): 113-121.

[35] Peng, X. Y., et al., Optimization analysis of ventilation simulation for meeting rooms in office buildings. Sichuan Building Science, 2023, 49(03): 89-97.

[36] Huang, T., et al., Simulation study on natural ventilation design of closed boiler room of coal-fired power plant in hot summer and warm winter area. Heating Ventilating & Air Conditioning, 2018, 48(9): 85-89.

[37] Wang, P., et al., Research on heat transfer and cooling capacity of buried tube radiant floor based on Fluent. Journal of Qingdao University of Technology, 2023, 44(02): 154-160.

[38] Shao, T., et al., Analysis of the Indoor Thermal Environment and Passive Energy-Saving Optimization Design of Rural Dwellings in Zhalantun, Inner Mongolia, China. Sustainability, 2020, 12(3).

[39] Liu, N., et al., Study on the influence of window-wall ratio on thermal comfort and system energy consumption of heating room. Refrigeration & Air Conditioning, 2023, 37(01): 66-72.

[40] Di, Y. H., et al., Numerical simulation of indoor thermal environment of movable slab house in a construction site based on Airpak. Journal of Xi'an Polytechnic University, 2023, 37(02): 40-46.

[41] Tian, X., et al., Stratified micro-environments using a sidewall air supply: An experimental and simulation study. Building and Environment, 2022, 224.

Submitted: 22.09.2023.
Revised: 10.01.2024.
Accepted: 30.07.2024.